Mass Detection Using Capacitive Resonant Silicon Resonator Employing LC Resonant Circuit Technique

Mass detection using capacitive resonant silicon resonator employing *LC* resonant circuit technique

Sang-Jin Kim,[a] Takahito Ono,[b] and Masayoshi Esashi
Graduate School of Engineering, Tohoku University, 6-6-01 Aza Aoba, Aramaki, Aoba-ku, Sendai 980-8579, Japan

(Received 8 February 2007; accepted 3 July 2007; published online 8 August 2007)

Capacitive resonant mass sensing using a single-crystalline silicon resonator with an electrical *LC* oscillator was demonstrated in ambient atmosphere. Using capacitive detection method, the detectable minimum mass of 1×10^{-14} g was obtained in the self-oscillation of cantilever with a thickness of 250 nm. The noise amplitude of the sensor output corresponds to a vibration amplitude of 0.05 nm/$(\mathrm{Hz})^{0.5}$ in the frequency domain compared with the actuation signal, which is equivalent to the detectable minimum capacitance variation of 2.4×10^{-21} F. Using the capacitive detection method, mass/stress induced resonance frequency shift due to the adsorption of ethanol and moist vapor in a pure N_2 gas as a carrier is successfully demonstrated. These results show the high potential of capacitive silicon resonator for high mass/stress-sensitive sensor. © *2007 American Institute of Physics.* [DOI: 10.1063/1.2766840]

I. INTRODUCTION

Mass sensors based on a micro-/nanomechanical resonator are expected to achieve extreme performance as required in chemical, environmental, medical fields,[1–8] in which only infinitesimal amount of specimens are available for analyses. The characterization of nanomaterials is one of the important applications of mass sensors, such as hydrogen storage capacity of a carbon nanotube bundle, placed at the apex of a cantilevered mass sensor.[6] Also a thermal mass desorption spectrum of a picogram sample was demonstrated with a heated silicon mass sensor;[9] such applications are some of the driving forces in the development of high-sensitive mass sensors, which can be achieved by recent developments in micro-/nanomachining technology. Recent accomplishments obtained by these mass sensors are that femtogram order mass detection has been achieved under ambient pressure and temperature using a bimetal silicon cantilever[5] and higher mass resolutions of 10^{-18}–10^{-21} g have been achieved in vacuum and in ultrahigh-vacuum pressure at cryogenic temperature.[6,7,10] These sensors employ shifts in fundamental resonance frequency of the resonator in a simple harmonic resonance mode in response to mass changes[11] and have the fundamental issues for improving the performance of sensor in air. In atmospheric pressure, the quality factor (Q factor) declines due to air damping.[12] Also, various noise sources including the thermomechanical noise and temperature fluctuation noise limit the resolution of mass detection.[13,14] Miniaturization of the resonator is an effective way to increase mass resolution with increasing the mass sensitivity. However, miniaturization of the resonator increases the temperature fluctuation noise, especially if its measurement method such as optical sensing generates heat and heat conduction.[15] From this point of view, capacitive sensing is less sensitive to temperature fluctuation noise than optical detection methods because it does not employ an optical source. In this contribution, we present and demonstrate the operation of a capacitive mass sensing with a very thin single-crystalline silicon resonator. Finally, we present the evaluation results of the real time mass sensing to moist vapor and ethanol vapor with N_2 as carrier gas in atmospheric pressure.

II. DESIGN AND PRINCIPLE OF MASS SENSOR

A. Design

Figure 1 shows the schematic illustration of the mass sensor. A thin single-crystalline silicon cantilever is used as a resonator with two opposite electrodes for capacitive readout and electrostatic actuation. For operating in various environments, a heater element is integrated in this sensor, which can change the temperature of the cantilever, as required. The mass sensor consists of two cantilevers. One is the mass-sensing cantilever and the other is the reference cantilever that compensates for drift and temperature variation on mass sensing. The opposite electrodes were fabricated on a Pyrex glass substrate chosen to reduce parasitic capacitance.

1. Mass sensitivity of microcantilever

The resonance frequency f_0 at the fundamental mode vibration of cantilever can be expressed as

$$f_0=\frac{1}{2\pi}\sqrt{\frac{k}{m^*}},\quad m^*=nm_b, \tag{2.1}$$

where k is the spring constant of the cantilever and m^* is the effective mass of the cantilever. The effective mass is proportional to the actual mass of the cantilever m_b, and n is the geometric parameter. For a rectangular beam, n is known to be 0.24.[16] From Eq. (2.1), it is obvious that the resonant

[a]Electronic mail: sjkim@mems.mech.tohoku.ac.jp
[b]Electronic mail: tono@cc.mech.tohoku.ac.jp

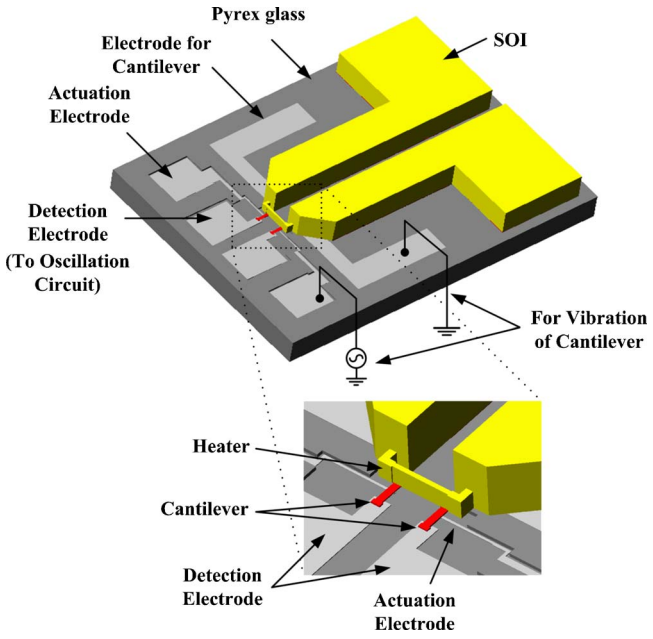

FIG. 1. (Color online) Schematic figure of the mass sensor which consists of two cantilevers (for mass detection and reference) and two opposite electrodes (for capacitive readout and electrostatic actuation).

frequency can change due to variation in mass and spring constant. The shift in resonance frequency can be written as

$$df(m^*,k) = \left(\frac{\partial f}{\partial m^*}\right)dm^* + \left(\frac{\partial f}{\partial k}\right)dk = \frac{f}{2}\left(\frac{dk}{k} - \frac{dm^*}{m^*}\right). \quad (2.2)$$

By designing cantilevers with localized adsorption area at the apex of the cantilever, the contribution to shift in resonance frequency due to differential surface stress [the dk/k term in Eq. (2.2)] can be minimized. Assuming that the contribution from the variation in the spring constant can be neglected, From Eq. (2.2), the shift of the fundamental resonance frequency can be written as

$$df(m^*,k) = \frac{f}{2}\left(-\frac{dm^*}{m^*}\right). \quad (2.3)$$

The resonant frequency is given by $f_0 = 0.162t\sqrt{E/\rho}/l^2$, where ρ is the density of the cantilever and E is the Young's modulus. t, w, and l are the thickness, width, and length of the cantilever, respectively. From Eqs. (2.1)–(2.3), mass sensitivity of cantilever in case of rectangular beam can be written as

$$\left|\frac{df}{dm^*}\right| = \frac{f}{2}\left(\frac{1}{m^*}\right) = 0.338\frac{1}{wl^3}\sqrt{\frac{E}{\rho^3}}. \quad (2.4)$$

As it can be seen from Eq. (2.4), the mass sensitivity increases in proportion to the decrease of the length and the width of cantilever. Therefore, high mass sensitivity can be obtained by miniaturizing the cantilever.

2. Quality factor in air

The resonance response of a cantilever is affected by various damping mechanisms such as air flow, squeeze effect, and clamping loss between support and cantilever, etc., when vibrating in atmospheric pressure. The Q factor takes into account these, and damping mechanisms can be expressed as follows:[3,7]

$$\frac{1}{Q} = \sum_i \frac{1}{Q_i} = \frac{1}{Q_{\text{air}}} + \frac{1}{Q_{\text{squeeze}}} + \frac{1}{Q_{\text{clamping}}} \approx \frac{6\pi\mu t}{\rho_s AL\omega_n} + \frac{\mu b^2}{\rho_s g_0^3 t\omega_n} + \frac{0.46t^3}{L^3}, \quad (2.5)$$

where L, b, t, ρ_s, ω_n, and A are the length, width, thickness, density, angular frequency, and cross sectional area of the cantilever, and μ and g_0 are the damping coefficient and the gap distance between the cantilever and the electrode. In Eq. (2.5), the first term points out the damping loss due to air flow in free space, which is inversely proportional to the specific length of the sensor according to a scaling law. The second term represents the damping loss caused by the squeeze effect, from scaling, which is mainly influenced by the gap distance. The last term indicates the damping due to clamping losses of cantilever, which is the elastic vibration of the supporting plate causing energy dissipation on vibrating cantilever. From this equation, it is found that the damping due to air flow in free space is dominant when the gap distance between cantilever and electrodes is on the order of micrometers.

3. Thermomechanical noise

As a resonator is in thermal equilibrium with its environment at a finite temperature, the mechanical vibration modes of resonator are coupled to thermal reservoir in terms of its thermodynamic energy and mechanically vibrate. This mechanical vibration of the resonator is referred to as thermomechanical noise that limits the resolution of the resonant mass sensor. The frequency fluctuation Δf_{noise} due to this thermomechanical vibration of the self-oscillated resonator is given by[11]

$$\langle(\Delta f_{\text{noise}})^2\rangle = \frac{f_0 k_B TB}{2\pi k Q\langle z_{\text{osc}}{}^2\rangle}, \quad (2.6)$$

where f_0, k_B, T, and B are the resonance frequency, Boltzmann constant, temperature of thermal reservoir, and bandwidth, respectively. Also k is the stiffness of the cantilever and $\langle z_{\text{osc}}{}^2\rangle$ is the mean-square vibration amplitude of the cantilever due to the thermal excitation. Using Eq. (2.6), the detectable minimum mass Δm_{min} estimated from the thermomechanical noise is expressed as follows:[9]

$$\Delta m_{\text{min}} = \frac{2G}{(\pi f_0)^{2.5}}\sqrt{\frac{kk_B TB}{\tau Q\langle z_{\text{osc}}{}^2\rangle}}, \quad (2.7)$$

where τ is the signal integration time and G is a value depending on its geometry of the cantilever. In the case that the mass is uniformly loaded on the rectangular cantilever, this factor is given by $G=1.37$. From scaling in Eq. (2.7), detectable minimum mass decreases with decreasing the size of the cantilever.

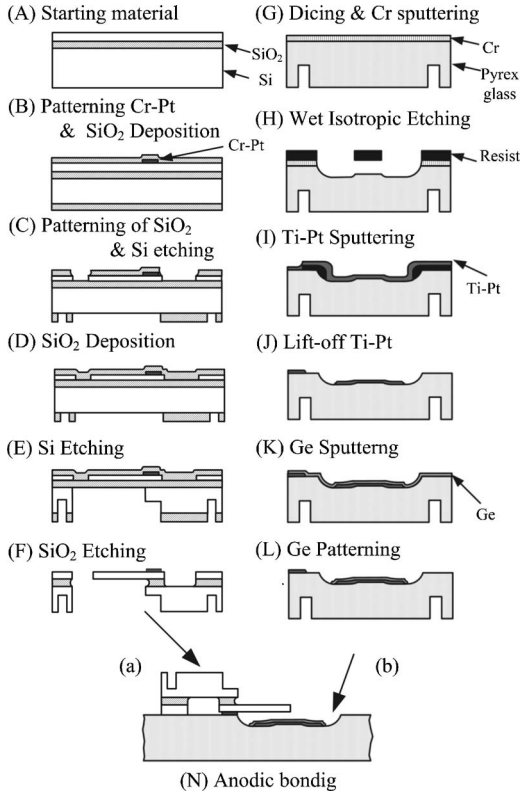

FIG. 2. Process flow for fabrication of mass sensor.

B. Principle of mass sensing

The designed capacitive mass sensor with silicon cantilevers as a resonator with capabilities of capacitive readout and electrostatic actuation is shown in Fig. 1. The electrical capacitance between the cantilever and the detection electrode is employed as the component of an electric *LC* Clapp oscillator with a high resonant frequency;[17] therefore, the resonant frequency of the *LC* oscillator depends on the capacitance of the sensor. Under the mechanical self-oscillation of the sensor, the resonant frequency of the *LC* oscillator is frequency modulated, and the vibration signal of the cantilever is obtained by demodulating its signal of the *LC* oscillator. The frequency change of mechanical resonance due to mass loading is measured using a frequency counter.

III. FABRICATION

As a starting material, boron-diffused silicon on insulator (SOI) wafer with a (100)-oriented *p*-type 250-nm-thick top silicon layer, 2-μm-thick intermediate SiO_2 layer, and 300-μm-thick handling layer was used. Figure 2 shows the process flow. 20-nm-thick Cr and 80-nm-thick Pt films were deposited on the wafer by sputtering and patterned by photolithography. A SiO_2 film with a thickness of 500 nm was formed by plasma-enhanced tetraethyl orthosilicate chemical vapor deposition (PE-TEOS CVD) on both sides of the wafer (B). The SiO_2 films on both sides were patterned by photolithography and wet etched in a buffered-HF (BHF) solution, and the cantilever pattern was defined by patterning the top silicon layer using a fast atom beam (FAB) of SF_6 (C). A 2-μm-thick SiO_2 film was deposited on the top side of silicon layer by PE-TEOS CVD and used as a stress compensation layer at the release process of cantilever (D). The substrate was etched from the back side with inductively coupled plasma reactive ion etching (ICP-RIE). In this step the heater element was fabricated (E). The cantilevers were released by wet etching of SiO_2 in HF (F). Figure 3 shows the magnified scanning electron microscope (SEM) image of cantilevers on the heating element. The thickness, length, and width of the cantilever were 250 nm, 67 μm, and 8 μm, respectively.

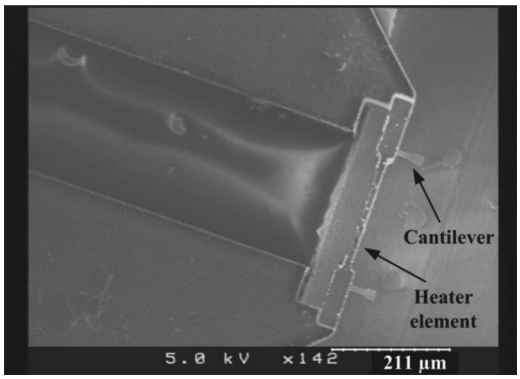

FIG. 3. Magnified SEM image of the fabricated cantilevers on the heating element.

A Pyrex glass substrate for making the opposite electrode was diced and Cr was deposited on the top side by sputtering (G). The Cr layer was patterned and the Pyrex glass substrate was isotropically etched in HF using the Cr layer as a mask (H). Ti and Pt layers with thicknesses of 20 and 80 nm, respectively, were deposited by sputtering and patterned by a lift-off process for making capacitive electrodes (I, J). Next, a Ge pattern as sacrificial layer for releasing the cantilevers was formed on the metal electrodes (K, L). The Pyrex glass substrate was bonded with the top silicon layer of the SOI wafer by anodic bonding (N). During this anodic bonding process, the cantilevers had often snapped onto the underlying electrode due to the electrostatic force. Therefore, the Ge layer on the electrode was employed as a sacrificial layer after the anodic bonding process. After the Ge was etched out in an etchant, the cantilevers were released. Finally, the cantilevers were released by supercritical point drying, and the fabrication process was completed. The magnified SEM image of the fabricated mass sensor is shown in Fig. 4. There are two electrodes at the opposite side of cantilever, one is the driving electrode with a 10 μm gap and the other one is the sensing electrode with a 7 μm gap.

IV. EXPERIMENTS

A. Frequency modulation (FM) using *LC* oscillator

As a resonator for mass sensor, the cantilever with a length, width, and thickness of 67 μm, 8 μm, and 250 nm, respectively, was evaluated. The fundamental resonant frequency of this resonator was approximately 78 kHz and the calculated spring constant of the beam is 0.02 N/m. Measured Q factor of the fundamental flexural mode was 10 in ambient pressure. A Clapp oscillator as the electrical oscillation circuit was adopted for capacitive displacement detection, in which the capacitive sensor was employed as the

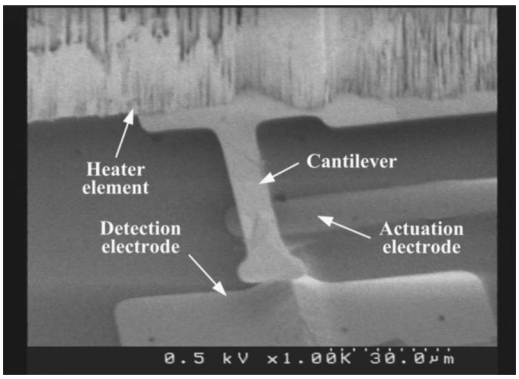

FIG. 4. Magnified SEM image of the fabricated mass sensor. The size of sensing electrode opposite to the cantilever with 7 μm gap distance was 15×18 μm^2, and its calculated capacitance is 3.4×10^{-16} F.

capacitive element of the *LC* oscillator, as shown in Fig. 5. The capacitance variation of the sensor modulates the resonant frequency of the oscillator circuit. Hence, the vibration signal was detected by a FM-demodulator circuit and feeds back to an actuator via a phase and gain adjuster, which self-oscillates the cantilever near the fundamental resonant frequency of 78 kHz. The oscillation frequency of the sensor was measured using a frequency counter. The resonant frequency from the oscillation circuit was approximately 1 GHz. The output signal of *LC* oscillation circuit is down converted to approximately 500 kHz by a mixer. From a spectrum analysis, the center frequency (ω_0) of the output signal of the *LC* oscillation circuit shifted to ω_0' due to the change of the average capacitance in vibration. Sideband peaks appeared at $\omega_0'-\omega_m$ and $\omega_0'+\omega_m$ because the *LC* oscillation circuit is modulated in the frequency domain by the vibration of the cantilever. Figure 6 shows the Fourier transform results of the frequency-modulated signal in mechanical vibration at the resonant frequency of 78 kHz; in these cases, the applied actuation voltages were 0 and 10 V. The noise amplitude of the sensor output was evaluated from the spectrum of FM-demodulated signal without the vibration of the cantilever. Simultaneously, actual vibration amplitude was measured by a laser Doppler vibrometer and compared with the output signal from the capacitive sensor. From this comparison, it was found that the noise amplitude of FM-demodulator corresponds to a vibration amplitude of

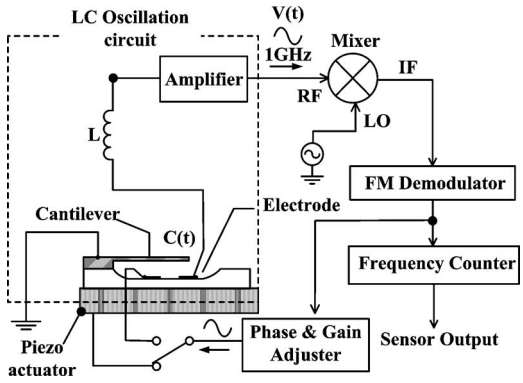

FIG. 5. Measurement system of the sensor employing Clapp oscillator as an *LC* oscillation circuit. FM demodulation was performed by Foster-Seeley discriminator.

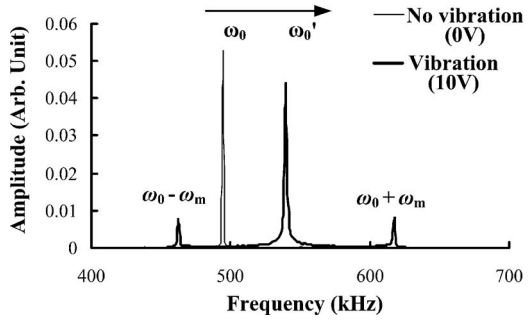

FIG. 6. Fourier transform results of the down-converted modulated signal, in the cases of the applied actuation voltages of 0 and 10 V with a vibration frequency of 78 kHz.

0.05 nm/(Hz)$^{0.5}$ in the frequency domain. The capacitance of the detection electrode with a gap of 7 μm is 3.4×10^{-16} F, and the vibrational noise amplitude is equivalent to the capacitance variation of 2.4×10^{-21} F.

B. Detectable minimum mass by capacitive detection

The advantage of the capacitive detection technique compared with an optical detection is less influenced by local heating effects and involved temperature fluctuation noise due to laser irradiation. The fluctuation of heat flow from the cantilever to the support and ambient atmosphere is the origin of the temperature fluctuation noise. In addition, the electrostatic force resulted from the charge fluctuation in the capacitance causes the mechanical vibration in capacitive detection method, but generally this effect is negligible under a low application voltage.

The detectable minimum mass based on capacitive detection using the identical cantilever beam was investigated from the frequency noise of the self-oscillated cantilever. The vibration amplitude $\langle z_{\mathrm{osc}}\rangle$ was adjusted to 230 nm. The setup for capacitive detection is shown in Fig. 5. The measurement was performed in ambient atmosphere at room temperature (~300 K) in a metal chamber. Figure 7 shows the detectable minimum mass measured by the capacitive detection as a function of the time constant of the signal integrating time in frequency detection.[17] The theoretical limit of detectable minimum mass originated in thermomechanical noise was calculated taking into account air damp-

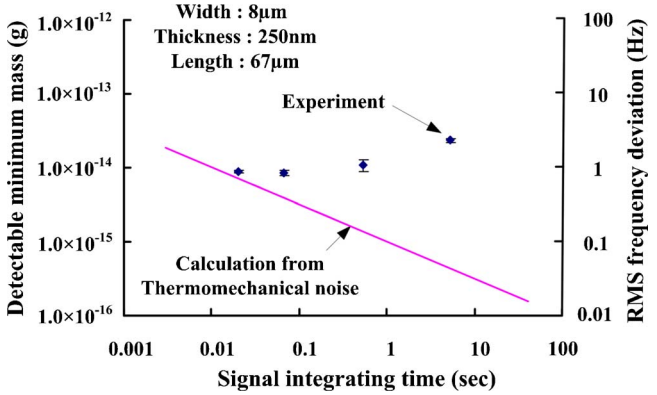

FIG. 7. (Color online) Detectable minimum mass of the piezoelectrically self-oscillated cantilever measured through capacitive detection as a function of the signal integrating time.

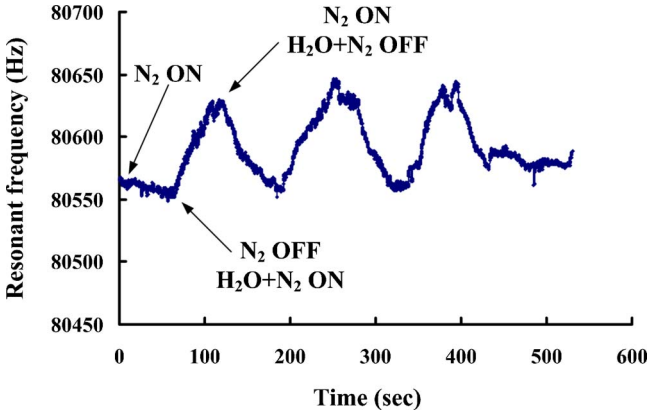

FIG. 8. (Color online) Measured real time shift in self-oscillation frequency by the adsorption and desorption of moist vapor.

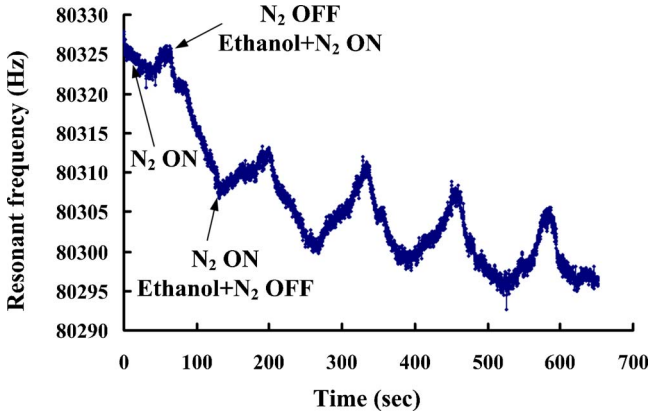

FIG. 9. (Color online) Measured real time shift in self-oscillation frequency by the adsorption and desorption of ethanol vapor.

ing and squeeze effect from Eq. (2.5) and plotted in Fig. 7.[18–20] The obtained detectable minimum mass of capacitive detection is close to that of calculated result at the short integration time of 0.02–0.08 s. Using this detection method in this cantilever, the detectable minimum mass of below 1×10^{-14} g was found to be attainable with a time constant of 0.08 s. As the signal integration time increases, the difference between experimental and theoretical values increases. This can be considered that flicker-type frequency fluctuation, which exhibits larger noise at smaller frequencies, is due to gas adsorption and desorption process on the surface of the mass sensor.[21] This adsorption and desorption noise depends on the adsorption energy of gas molecules on surface, pressure and temperature of environment, and influence the detectable minimum mass of sensor in actual use in ambient atmosphere.[21] However, in order to identify the dominant noise mechanism exactly, further investigations are necessary.

C. Mass measurement by capacitive detection

The evaluation on mass sensing was performed by detecting the infinitesimal mass of moist vapor in a carrier gas of N_2. The mass sensor with a spring constant of 0.02 N/m was used in this measurement. Natural silicon dioxide exists on the surface of silicon cantilever which will adsorb moist vapor. In order to measure the mass of moist vapor, the mass sensor which is placed inside a chamber filled with atmospheric pressure of dry N_2 was exposed to the humidified N_2 gas and dry N_2 gas alternately. The humidified N_2 gas was supplied into chamber via a bubbling reservoir filled with water at room temperature. The flow rate of carrier gas into chamber was 0.5 ℓ/min. The humidity of the output stream was monitored by a hygrometer and the concentration of moist vapor was 1400 ppm. Figure 8 shows the measurement results of the real time frequency variation in self-oscillation frequency when repeating adsorption and desorption of moist vapor. The resonant frequency increases by exposing humidified N_2 gas, and following exposure of pure N_2 to the sensor decreases the resonant frequency. This increase in resonant frequency is due to the surface stress originated in the physisorption of moist vapor on the surface of the cantilever, and the decrease in the resonant frequency is due to relaxation of surface stress stem from the desorption of moist vapor in the exposure of N_2. These resonance frequency shift caused by surface stress of adsorption layer on the sensor surface can also be found in other paper.[16,22,23] The adsorption induced surface stress on both sides of natural oxide layers on the cantilever does not generate the deflection originated from the unbalanced stress between the upper and the bottom surface but induces a deformation in the cantilever due to the longitudinal stress. This longitudinal stress causes the change of resonant frequency. The resulting resonant frequency can be calculated by the following equation:[22]

$$f_{\text{stress}} = f_0 \sqrt{1 - \sigma(60l^2/7Et^3)}, \tag{4.1}$$

where f_0 and σ are the resonance frequency and adsorption induced surface stress, respectively. l and t are the cantilever length and thickness, respectively. From Eq. (4.1), the resonance frequency increase of 70 Hz corresponds to the tensile stress of 9.54×10^{-5} N/m. In this calculation, l is 67 μm, t is 250 nm, and f_0 is 78 kHz. The mass sensing for ethanol vapor in a carrier gas of N_2 was performed as well using the same mass sensor with the same measurement setup. The flow rate of carrier gas into chamber was 1 ℓ/min. Figure 9 shows the measurement results when repeating the adsorption and desorption of ethanol vapor. In contrast to water vapor, the resonance frequency decreases by exposing ethanol gas with N_2 carrier gas and increases by exposure of pure N_2. These results normally show the mass loading and unloading on resonator due to the adsorption and desorption of ethanol vapor.

V. DISCUSSION

Single-crystalline silicon resonators as a mass sensor with capabilities of capacitive readout and electrostatic actuation were presented and demonstrated. In the self-oscillated cantilever with a thickness of 250 nm, the detectable minimum mass of 1×10^{-14} g was obtained using the capacitive detection method in air. The noise amplitude of the sensor output corresponds to vibration amplitude of 0.05 nm/$(\text{Hz})^{0.5}$ in the frequency domain in comparison with the actuation signal, which is equivalent to the detectable minimum capacitance variation of 2.4×10^{-21} F. Using this capacitive detection method, mass/stress induced resonance

frequency shift due to the adsorption of ethanol and moist vapor by using pure N_2 gas as a carrier was successfully demonstrated. In the case of ethanol, the mass loading effects caused by the adsorption and desorption of ethanol vapor on sensor surface were observed, whereas, in the case of moist vapor, the resonant frequency increased due to the surface stress caused by the physisorption of moist vapor on the surface. These results show the high potential ability of capacitive silicon resonator for high mass/stress-sensitive sensor.

ACKNOWLEDGMENTS

Part of this work was performed in the Micro/Nanomachining Research and Education Center of Tohoku University. This work was supported in part by a Grant-in Aid for Scientific Research from the Ministry of Education, Culture, Sports, Science, and Technology of Japan.

[1] A. Gupta, D. Akin, and R. Bashir, Appl. Phys. Lett. **84**, 1976 (2004).
[2] F. M. Battiston, J. P. Ramseyer, and H. P. Lang, Sens. Actuators B **77**, 122 (2001).
[3] B. Ilic, D. Czaplewski, M. Zalalutdinov, and H. G. Craighead, J. Vac. Sci. Technol. B **19**, 2825 (2001).
[4] H. Jensenius, J. Thaysen, A. A. Rasmussen, L. H. Veje, O. Hansen, and A. Boisen, Appl. Phys. Lett. **76**, 2615 (2000).
[5] N. V. Lavrik and P. G. Datskos, Appl. Phys. Lett. **82**, 2697 (2003).
[6] T. Ono, X. Li, and H. Miyashita, Rev. Sci. Instrum. **74**, 1240 (2003).
[7] K. L. Ekinci, X. M. H. Huang, and M. L. Roukes, Appl. Phys. Lett. **84**, 4469 (2004).
[8] E. Forsen *et al.*, Appl. Phys. Lett. **87**, 043507 (2005).
[9] T. Ono and M. Esashi, Meas. Sci. Technol. **15**, 1997 (2004).
[10] Y. T. Yang, C. Callegari, X. L. Feng, K. L. Ekinci, and M. L. Roukes, Nano Lett. **6**, 583 (2006).
[11] T. R. Albrecht, P. Grütter, D. Horne, and D. Rugar, J. Appl. Phys. **69**, 668 (1991).
[12] K. Y. Yasumura, T. D. Stowe, E. M. Chow, T. Pfafman, T. W. Kenny, B. C. Stipe, and D. Rugar, J. Microelectromech. Syst. **9**, 117 (2000).
[13] A. N. Cleland and M. L. Roukes, J. Appl. Phys. **92**, 2758 (2002).
[14] K. L. Ekinci, Y. T. Yang, and M. L. Roukes, J. Appl. Phys. **95**, 2682 (2004).
[15] J. R. Vig and Y. Kim, IEEE Trans. Ultrason. Ferroelectr. Freq. Control **46**, 1558 (1999).
[16] G. Y. Chen, T. Thundat, E. A. Wachter, and R. J. Warmack, J. Appl. Phys. **77**, 3618 (1995).
[17] S. J. Kim, T. Ono, and M. Esashi, Appl. Phys. Lett. **88**, 053116 (2006).
[18] H. Hosaka and K. Itao, Sens. Actuators, A **49**, 87 (1995).
[19] F. R. Blom, S. Bouwstra, M. Elwenspoek, and J. H. J. Fluitman, J. Vac. Sci. Technol. B **10**, 19 (1992).
[20] L. D. Landau and E. M. Lifshitz, *Fluid Mechanics*, 2nd ed., Course of Theoretical Physics Vol. 6 (Pergamon, Oxford, 1963).
[21] Y. K. Yong and J. R. Vig, IEEE Trans. Ultrason. Ferroelectr. Freq. Control **37**, 543 (1990).
[22] T. Ono, D. F. Wang, and M. Esashi, Appl. Phys. Lett. **83**, 1950 (2003).
[23] J. Lagowski, H. C. Gatos, and E. S. Sproles, Jr., Appl. Phys. Lett. **26**, 493 (1975).